Rotational Resonance NMR Determination of Intra- and Intermolecular Distance Constraints in Dipalmitoylphosphatidylcholine Bilayers†

Steven O. Smith*

Department of Molecular Biophysics and Biochemistry, Yale University, New Haven, Connecticut 06520-8114

James Hamilton and Amir Salmon

Department of Biophysics, Boston University, Boston, Massachusetts 02118

Barbara J. Bormann

Boehringer-Ingelheim, Ridgefield, Connecticut 06877

Received December 3, 1993; Revised Manuscript Received March 10, 1994®

ABSTRACT: Rotational resonance (RR) NMR methods are explored for determining intramolecular and intermolecular distances between ^{13}C-labeled sites in membrane bilayers. Specific ^{13}C labels have been incorporated into dipalmitoylphosphatidylcholine (DPPC) and a hydrophobic peptide corresponding to the transmembrane domain of human glycophorin A. The exchange of magnetization between these labels in the RR NMR experiment can be related to their internuclear separation. Intramolecular magnetization exchange rates have been measured between ^{13}C labels incorporated at the 1-position of the *sn*-1 acyl chain (1-[1-^{13}C]) and the 2-position of the *sn*-2 acyl chain (2-[2-^{13}C]) of DPPC. These positions are 5.3–5.5 Å apart in the crystal structure of dimyristoylphosphatidylcholine (DMPC), but are estimated to be 4.5–5.0 Å apart in DPPC below the subphase transition temperature. These results are consistent with a smaller axial displacement between the *sn*-1 and *sn*-2 acyl chains than the ~3.6-Å displacement observed in the DMPC crystal structure. Intermolecular magnetization transfer rates have been measured between 1,2-[2-^{13}C]DPPC and 2-[1-^{13}C]DPPC and between 1,2-[1-^{13}C]DPPC and 2-[2-^{13}C]DPPC. In addition, intermolecular magnetization exchange rates have been measured between 1,2-[2-^{13}C]DPPC and the ^{13}C–OH position of Y_{93} in the glycophorin transmembrane domain. These intermolecular distance measurements demonstrate that the relative orientation and location of membrane lipids and peptides can be established using RR NMR methods.

Phospholipids are the major structural constituents of most biomembranes, and the crystal structures of several phospholipid molecules have served for years as an important reference for lipid structure in hydrated membrane bilayers [see Pascher et al. (1992)]. These structures have provided high-resolution structural detail that has previously not been possible to obtain by other approaches and have yielded insights into the molecular conformations and the packing arrangements of the lipid head groups and hydrocarbon chains. However, the correlation between lipid structure in single crystals and the structure of heterogeneous membrane bilayers has generally been made by lower resolution methods. Recently, magic angle spinning NMR methods have been developed for measuring internuclear distances in membrane proteins and peptides, and the 0.2–0.5-Å resolution that can be attained is comparable to or exceeds that in diffraction measurements (Thompson et al., 1992; Smith & Peersen, 1992; Smith et al., 1994). These methods open up the possibility of direct structural studies on fully hydrated lipids in multicomponent membrane systems.

Membrane samples generally yield broad unresolved NMR resonances because of chemical shift anisotropy and dipolar interactions (Griffin, 1981; Smith & Peersen, 1992). Magic angle spinning (MAS)[1] mechanically averages these interactions, yielding high-resolution NMR spectra consisting of narrow center-bands at the isotropic chemical shift and rotational side-bands spaced by the MAS frequency. Rotational resonance (RR) NMR is a MAS method that *selectively* restores weak homonuclear dipolar couplings between two nuclear spins that have different chemical shifts by spinning the sample such that a multiple of the MAS speed (ω_r) matches the frequency difference ($\Delta\omega$) between the two spins ($\Delta\omega = n\omega_r$) (Raleigh et al., 1988; Levitt et al., 1990; Peersen & Smith, 1993). The measured dipolar coupling (D) is related to the internuclear distance (r) between the spins by the simple relationship $D = \hbar\gamma^2 r^{-3}$, where $\hbar$ is Planck's constant and γ is the nuclear gyromagnetic ratio. We have shown in crystals of a hydrophobic peptide that RR NMR measurements can yield $^{13}C\cdots{}^{13}C$ distances up to ~6.5 Å (Peersen et al., 1992). The resolution depends on the internuclear separation but is better than 0.3 Å when the $^{13}C\cdots{}^{13}C$ distances are ~5 Å or less.

The RR NMR experiments can be designed to address lipid structure through the measurement of *intramolecular* magnetization exchange rates between isolated $^{13}C\cdots{}^{13}C$ pairs. In this study, intramolecular RR NMR measurements are made between ^{13}C sites on the acyl chains of dipalmitoylphos-

† This research was supported by the National Institutes of Health (GM-41412), the American Cancer Society (BE-138), and the Searle Scholars Program/Chicago Community Trust.

* To whom correspondence should be addressed.

® Abstract published in *Advance ACS Abstracts,* April 15, 1994.

[1] Abbreviations: CPMG, Carr–Purcell Meiboom–Gill; DMPC, dimyristoylphosphatidylcholine; DPPC, dipalmitoylphosphatidylcholine; GPA-TM, glycophorin A transmembrane; MAS, magic angle spinning; RR NMR, rotational resonance nuclear magnetic resonance spectroscopy; VACP, variable-amplitude cross polarization.

0006-2960/94/0433-6327$04.50/0

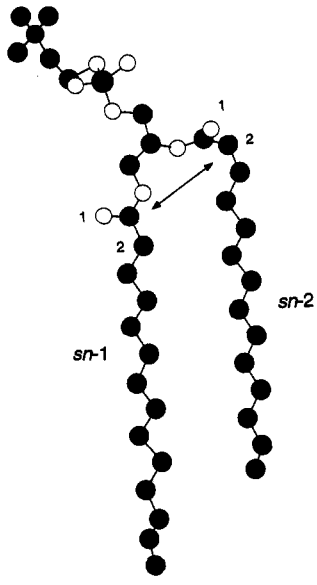

FIGURE 1: Crystal structure of dimyristoylphosphatidylcholine (Pearson & Pascher, 1979). The distance between the *sn*-1 $^{13}C{=}O$ and the *sn*-2 $^{13}CH_2$ is 5.52 Å. The DMPC structure is of molecule A in the asymmetric unit cell.

phatidylcholine (DPPC). Specific ^{13}C labels have been incorporated into DPPC at the carbonyl of the *sn*-1 acyl chain and the 2-methylene of the *sn*-2 acyl chain. The distances between these sites in the crystal structure of DMPC, where there are two molecules in the asymmetric unit cell, are 5.52 Å (molecule A, Figure 1) and 5.34 Å (molecule B). In the DMPC structure, the glycerol backbone is roughly perpendicular to the bilayer plane, and the acyl chains are displaced relative to one another by ~3.6 Å (Pearson & Pascher, 1979). The crystal structure of DPPC has not been determined, although neutron diffraction studies of DPPC in gel-phase membranes indicate that the axial displacement is ~1.8 Å, corresponding to about 1.5 methylene units (Büldt et al., 1978). The intramolecular distance between the two ^{13}C sites indicated in Figure 1 is sensitive to the interfacial conformation of DPPC and provides an independent measure of the structure of DPPC in hydrated membranes.

RR NMR measurements of *intermolecular* magnetization exchange between ^{13}C labels on different membrane components can also be made to characterize lipid–lipid and lipid–protein interactions. We have explored the potential of using intermolecular RR NMR for establishing structural constraints in membranes by measuring intermolecular magnetization exchange rates between specific ^{13}C labels on different DPPC molecules and between ^{13}C-labeled DPPC and a hydrophobic peptide corresponding to the transmembrane domain of glycophorin A (GPA-TM). Glycophorin spans the membrane in a single α-helical stretch of 23 mostly hydrophobic amino acids with the transmembrane region terminating in charged glutamate or arginine residues.

P-E-I-T-L-I-I-F-G-V-M-A-G-V-I-G-T-I-L-L-I-S-
Y_{93}-G-I-R-R

Marchesi and co-workers first demonstrated that the transmembrane domain is responsible for dimerization of the protein (Furthmayr & Marchesi, 1976; Bormann et al., 1989). Recently, mutagenesis and computational studies have shown that L_{76}, I_{77}, G_{79}, G_{83}, and T_{87} are in the dimer interface (Lemmon et al., 1992a,b; Treutlein et al., 1992). Rotational resonance NMR measurements have been undertaken (Smith et al., 1994) to determine the local secondary structure of the GPA-TM domain. These studies are extended in this paper to the lipid–protein interface where we have targeted Y_{93}. Y_{93} is thought to be oriented toward the surrounding lipids and near the membrane interface when the protein is in a helical geometry (Lemmon et al., 1992a,b; Treutlein et al., 1992).

MATERIALS AND METHODS

The synthesis of ^{13}C-labeled DPPC has been described previously (Smith et al., 1992). Briefly, 1,2-[1-^{13}C]DPPC and 1,2-[2-^{13}C]DPPC were prepared by acylation of the cadmium complex of L-α-glycerophosphorylcholine (Sigma, grade I) with [1-^{13}C]- or [2-^{13}C]palmitic acid (Cambridge Isotopes, Woborn, MA) in chloroform. Reaction conditions were used to maximize the yield based on the fatty acid. 2-[1-^{13}C]DPPC and 2-[2-^{13}C]DPPC were prepared in a similar fashion by acylation of lysopalmitoylphosphatidylcholine with [1-^{13}C]- or [2-^{13}C]palmitic acid. Lipid samples for NMR were prepared by mixing the appropriate amounts of lipids in chloroform, codrying the lipids under nitrogen, and removing trace amounts of organic solvent under high vacuum for at least 1–2 h. For the intramolecular DPPC measurements, 1-[1-^{13}C],2-[2-^{13}C]DPPC (~5 mg) was diluted 1:6 with unlabeled DPPC (Avanti Polar Lipids, Alabaster, AL) in order to reduce intermolecular transfer. For the intermolecular measurements, 2-[2-^{13}C]DPPC was mixed in a 1:10 ratio with 1,2-[1-^{13}C]DPPC or 2-[1-^{13}C]DPPC was mixed in a 1:10 ratio with 1,2-[2-^{13}C]DPPC. Phospholipids were dispersed by bath sonication in phosphate buffer (10 mM KH_2PO_4, pH 7, and 150 mM NaCl) and pelleted in an ultracentrifuge. The fully hydrated multilamellar dispersions were loaded into a 5-mm-diameter rotor for the MAS NMR experiments. The samples were typically stored for several weeks below the DPPC subphase transition temperature before final NMR measurements were made. No significant differences in the magnetization exchange rates were observed for those measurements made immediately after packing the NMR rotor, suggesting that the excess hydration did not allow formation of the low-temperature crystal phase of the lipid (Ruocco & Shipley, 1982; Nagle & Wilkinson, 1982).

The L-[4′-^{13}C]tyrosine was obtained from Cambridge Isotopes (Cambridge, MA) and N-protected as the *tert*-butyl carbamate derivative by standard methods (Roeske, 1963) at Boehringer Ingelheim. The 29 amino acid GPA-TM peptides were synthesized at the Protein and Nucleic Acid Chemistry Facility at Yale and purified by reverse-phase HPLC on a semipreparative Vydac C4 column using an acetonitrile/2-isopropanol/water gradient (Smith et al., 1994). The peptides were further characterized by mass spectroscopy and quantitated by amino acid analysis. Reconstitution of the GPA-TM peptides into either ^{13}C-labeled or unlabeled DPPC was performed by detergent dialysis. DPPC and pure peptide (~5 mg) were separately dissolved in 2% octyl β-glucoside, combined in a 20:1 molar ratio, and sonicated. The octyl β-glucoside was dialyzed using Spectra-Por 3 dialysis tubing (3000 MW cutoff) for 1–2 days against phosphate buffer. The peptide-containing vesicles were concentrated, further purified by sucrose gradient centrifugation (20–70%), washed several times to remove the sucrose, and pelleted.

^{13}C NMR spectra were obtained at 90.4 MHz on a Chemagnetics CMX spectrometer using a 5-mm high-speed double-resonance probe from Doty Scientific (Columbia, SC). The pulse sequence used for the RR experiments is shown in Figure 2 and was similar to that described previously (Peersen et al., 1992). Variable-amplitude cross polarization (VACP) used during the contact period yields several advantages in

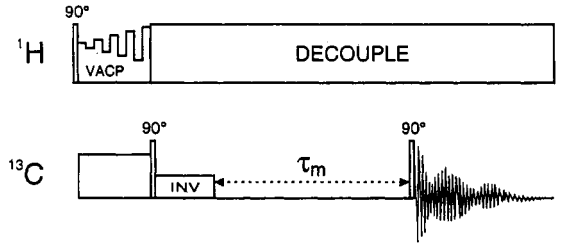

FIGURE 2: Pulse sequence for rotational resonance NMR experiments incorporating variable-amplitude cross polarization. The carbon magnetization generated by cross polarization is stored on the z-axis with a 90° pulse, and one of the two spins being studied is then selectively inverted with a low-power pulse. The spins are then allowed to exchange Zeeman magnetization during a variable mixing time (τ_m), and the distribution of signal at the end of this period is sampled with a 90° read pulse.

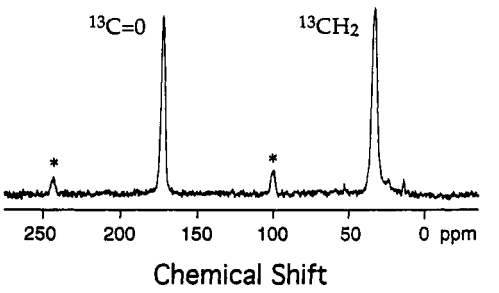

FIGURE 3: MAS NMR spectrum of 1-[1-^{13}C],2-[2-^{13}C]DPPC obtained at a MAS frequency of 6.5 kHz. The ^{13}C=O and ^{13}CH$_2$ resonances are separated by 12 496 Hz. Rotational sidebands of the ^{13}C=O resonance are marked with asterisks. The temperature was maintained at −50 °C.

the RR experiment over conventional CP (Peersen et al., 1993; 1994). The VACP sequence reduces the sensitivity of cross polarization to the Hartmann–Hahn matching condition under high MAS speeds, where a mismatch of 2–4 kHz in the spin-lock frequencies can severely reduce CP efficiency. As a result, the absolute intensities of the resonances being monitored in the RR experiment are less sensitive to small changes in amplifier output and probe tuning. This stability is critical in obtaining reliable intensities in RR NMR spectra that require long data acquisitions. VACP also compensates for inhomogeneous B_1 fields leading to an increase in signal in the CP experiment (Peersen et al., 1994). The proton power was adjusted for a 3-μs 90° pulse length and then modulated during the VACP contact time. The decoupling power was returned to a field strength of 83 kHz during the variable delay and acquisition. The amount of magnetization exchange is dependent on the decoupling power (Peersen & Smith, 1993; O. B. Peersen, S. Aimoto, and S. O. Smith, in preparation). A series of magnetization exchange curves for 1-[1-^{13}C],2-[2-^{13}C]DPPC obtained at ^{1}H field strengths ranging from 50 to 130 kHz show that the curves begin to merge in the range of 70–80 kHz.

The pulse sequence used to estimate the inhomogeneous contribution to the line widths in the MAS spectrum was based on the method of Garroway (Garroway, 1977). Standard proton cross polarization generates ^{13}C magnetization in the transverse plane that is allowed to dephase for a time τ after the ^{13}C spin-lock pulse. A CPMG train of ^{13}C π-pulses is then applied at a spacing of 2τ to produce a train of spin echoes while decoupling on the proton channel. Fourier transformation of the echo train produces a spectrum of uniformly spaced lines at $(2\tau)^{-1}$. The observed line widths in the echo-train spectrum reflect the homogeneous contribution to the T_2.

The intramolecular magnetization exchange curves were generated by integration of the methylene and carbonyl peaks. The natural abundance intensity contributing to each resonance was calculated by counting the number of background carbons in DPPC and accounting for the 1.1% ^{13}C natural abundance. The first two time points in the RR series (100 μs and 1 ms) were averaged and normalized to 1.0. Simulations of the magnetization exchange curves were performed using the methods of Levitt et al. (1990). The simulations depend on several parameters *in addition to* the internuclear distance. These include the orientation and chemical shift anisotropy (CSA) tensor of each spin, as well as zero quantum T_2 relaxation, which accounts in a global way for several processes influencing magnetization exchange not driven by rotational resonance. The chemical shift tensors for the C=O and CH_2 groups are taken from studies on alanylalanine and glycine, respectively (Hartzell et al., 1987; Oas et al., 1987; Haberkorn et al., 1981). The dependence of magnetization exchange on both the CSA and the tensor orientations is minor when the sample is spinning at the $n = 1$ rotational resonance condition.

RESULTS AND DISCUSSION

Intramolecular RR NMR Measurements. The first set of RR NMR experiments were on DPPC specifically ^{13}C-labeled at two sites on the same molecule and consequently at a relatively fixed distance apart. The MAS spectrum of 1-[1-^{13}C],2-[2-^{13}C]DPPC in Figure 3 is dominated by the two ^{13}C resonances that are separated in frequency ($\Delta\omega$) by 12 496 Hz. Rotational sidebands (marked with asterisks) are spaced at the MAS frequency (ω_r) of 6.5 kHz from the ^{13}C carbonyl centerband. This is slightly higher than the $n = 2$ resonance condition ($\Delta\omega = 2\omega_r$). Figure 4 presents RR NMR spectra of 1-[1-^{13}C],2-[2-^{13}C]DPPC at −50 °C (a) and 5 °C (b). Lipid motion is restricted at these temperatures, which are well below the phase transition temperature of DPPC (42 °C). Motional averaging in the RR NMR experiment leads to a reduction in the observed RR exchange rate and a longer estimate for the internuclear distance. The spectra in Figure 4 were obtained at a MAS frequency of 6248 Hz, corresponding to the $n = 2$ resonance condition. In both cases, the ^{13}C=O resonance was inverted and offset plots of only the ^{13}C=O and ^{13}CH$_2$ resonances are shown as a function of the variable RR exchange time. The RR-driven decrease of intensity is clearly observed in both of the resonances. As the temperature is increased from −50 to 5 °C, the ^{13}C resonances gradually narrow from 237 Hz (C=O) and 317 Hz (CH_2) to 127 Hz (C=O) and 182 Hz (CH_2); however, the extent of magnetization exchange remains roughly the same.

The dipolar coupling between the two ^{13}C labels can be estimated from the intensity changes observed in the RR experiment. Figure 5 presents magnetization exchange curves generated from the difference in peak intensity (CH_2—C=O) as a function of the mix time. The $n = 1$ resonance curves in Figure 5a were obtained at 12 496 Hz for 1-[1-^{13}C],2-[2-^{13}C]DPPC and 1-[1-^{13}C]DPPC. There is a rapid drop in intensity for the doubly ^{13}C-labeled DPPC (●), reflecting strong coupling between the two ^{13}C labels. The singly ^{13}C-labeled DPPC curve (■) serves as a control to estimate the contribution to the measured exchange curves from dipolar coupling to natural abundance ^{13}C, which is about 5%. Finally, off rotational resonance spectra were obtained for 1-[1-^{13}C],2-[2-^{13}C]DPPC (□). These experiments serve as a baseline for quantitating the extent of RR-driven exchange. It is possible to observe changes in intensity of the ^{13}C resonances due to changes in probe tuning or sample temperature as the variable mix time and length of proton decoupling are increased. The

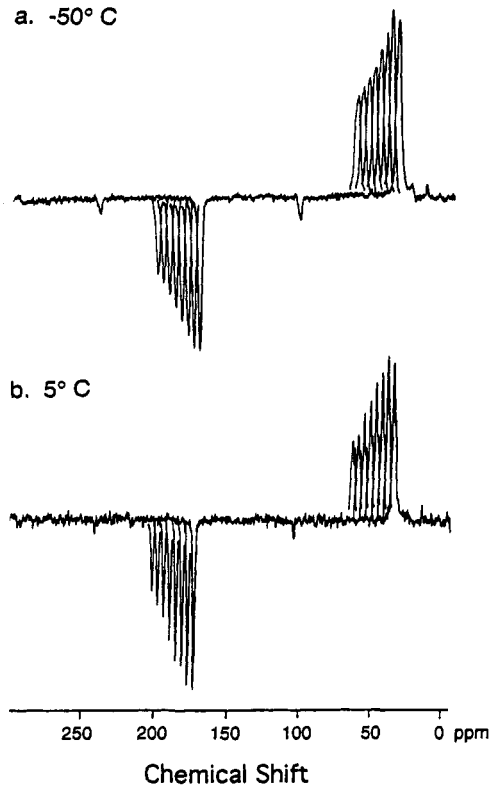

FIGURE 4: Rotational resonance NMR spectra at the $n = 2$ resonance condition for 1-[1-^{13}C],2-[2-^{13}C]DPPC at −50 °C (a) and 5 °C (b). The full spectrum is shown for the initial mix time of 100 μs along with offset plots of the ^{13}C resonances for mix times of 1, 5, 10, 20, 30, 40, and 50 ms. The MAS frequency was maintained at 6248 ± 5 Hz. Each spectrum is the average of 1024 scans and was processed with 30-Hz exponential line broadening. The recycle delay was 2.5 s.

VACP sequence minimizes the influence of probe tuning and amplifier stability on the ^{13}C intensities, while low temperature reduces the effects of proton decoupling. We have found that above ~15 °C the sample temperature can change substantially due to the high-power decoupling pulse, resulting in large changes in the intensities of the lipid resonances. The $n = 2$ magnetization exchange curves for 1-[1-^{13}C],2-[2-^{13}C]-DPPC are shown in Figure 5b,c.

The experimental data in Figure 5 are presented along with a series of simulations showing calculated magnetization exchange curves using dipolar couplings corresponding to internuclear distances between 3.5 and 5.5 Å. For the $n = 1$ exchange curves, the experimental data track the 4.0-Å simulation. Comparison between the simulated curves and the scatter in the data points shows that the *precision* in the measurements is on the order of 0.2 Å at this distance. The $n = 2$ measurements (Figure 5b,c) are best fit by simulated curves between 3.8 and 4.2 Å. The *accuracy* of the measurements is dependent on the accuracy of the input parameters used in the simulation program in addition to the experimental design and the generation of the magnetization exchange curves. We have discussed the experimental aspects of the RR measurements briefly above and in more detail elsewhere (Peersen & Smith, 1993; O. B. Peersen, S. Aimoto, and S. O. Smith, in preparation).

The $n = 1$ exchange curves are largely insensitive to the orientations of the chemical shift and dipolar tensors; however, uncertainty in the tensor orientations in the $n = 2$ simulations translates into an uncertainty in the distance estimates of ~0.5 Å. A similar uncertainty in the simulated curves is generated by an uncertainty in the value of the zero-quantum

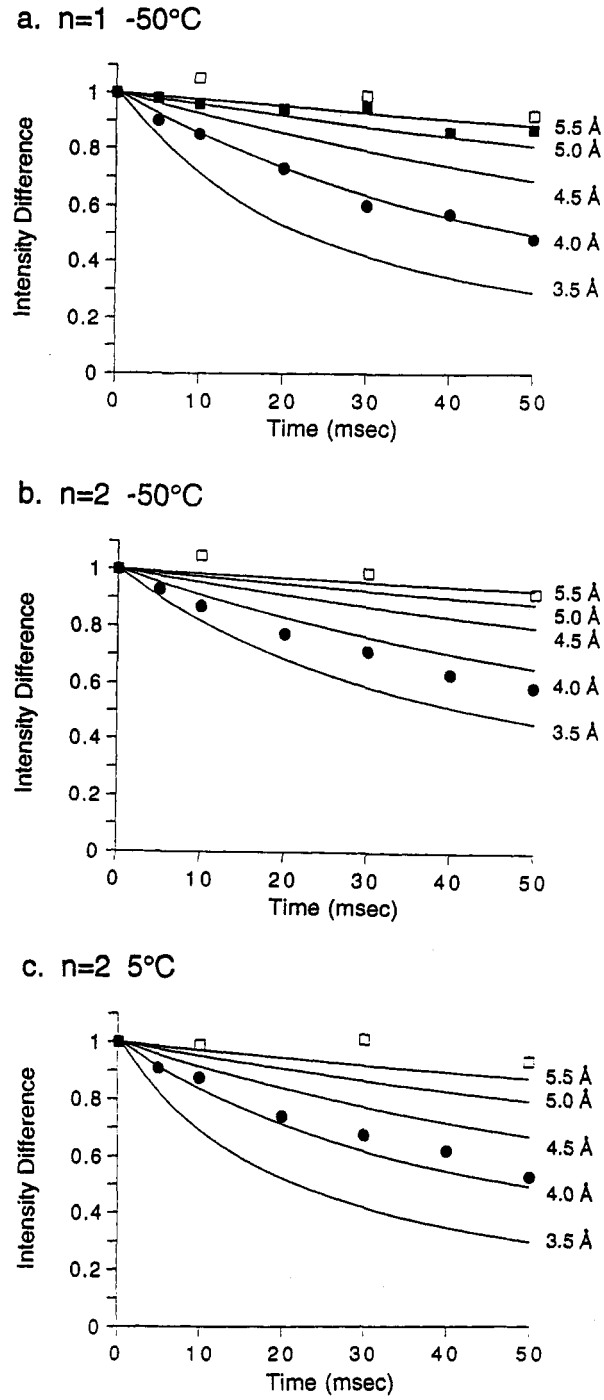

FIGURE 5: Magnetization exchange curves and simulations for intramolecular RR measurements in DPPC. (a) On rotational resonance ($n = 1$) experimental data for 1-[1-^{13}C],2-[2-^{13}C]DPPC (●) and 1-[1-^{13}C]DPPC (■) at −50 °C. Off resonance data (□) on 1-[1-^{13}C],2-[2-^{13}C]DPPC was obtained at 9 kHz. Simulations (—) for a series of distances are shown using a T_2^{ZQ} of 600 μs. (b) On (●) and off rotational resonance (□) ($n = 2$) data for 1-[1-^{13}C],2-[2-^{13}C]DPPC obtained at −50 °C. Simulations for a series of distances are shown using a T_2^{ZQ} of 600 μs. (c) On (●) and off rotational resonance data (□) ($n = 2$) for 1-[1-^{13}C],2-[2-^{13}C]DPPC obtained at 5 °C. Simulations for a series of distances are shown using a T_2^{ZQ} of 1.0 ms.

T_2 relaxation. This term will shift *both* the $n = 1$ and $n = 2$ simulations. Increasing the value of the zero-quantum relaxation leads to more rapid exchange of magnetization in the simulations and results in a longer estimate of the internuclear distance. For the simulations shown in Figure 5, the value of the zero-quantum relaxation term was estimated from the line widths (Δ) using the relationship $T_2 = 1/\pi$-

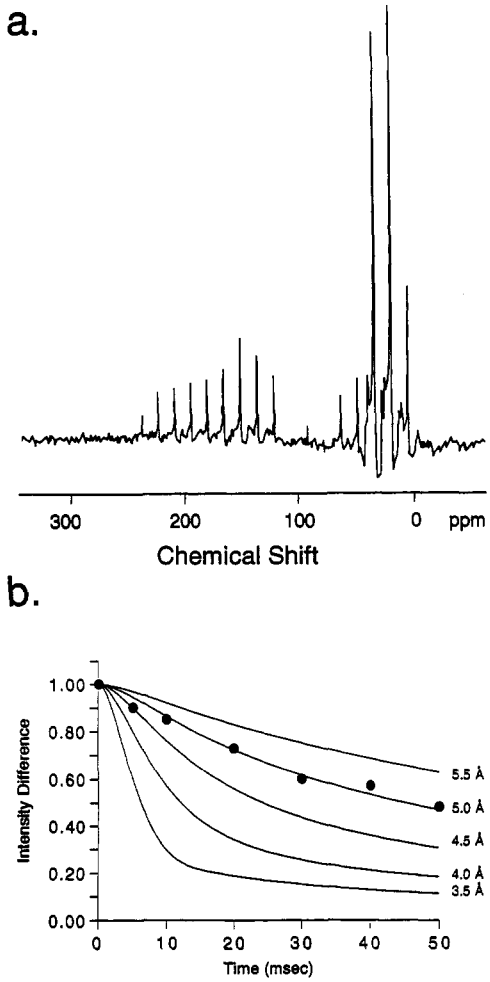

FIGURE 6: (a) ^{13}C NMR echo-train spectrum of 1-[1-^{13}C],2-[2-^{13}C]DPPC obtained at −50 °C without MAS. The spectrum is the average of 512 scans and was processed without exponential line broadening. (b) Comparison of the experimental −50 °C $n = 1$ magnetization exchange curve with simulations using a T_2^{ZQ} of 2.1 ms.

($\Delta C{=}O + \Delta CH_2$). This expression is derived from the work of Kubo and McDowell (1988), which indicates that the zero-quantum relaxation rate of a homonuclear spin pair can be obtained from the single-quantum relaxation rates of the two spins. Griffin and co-workers have argued that estimates based on the line widths are reliable for obtaining accurate distances from simulations of the magnetization exchange curves (Thompson et al., 1992).

One important contribution to the observed line width that would lead to an overestimate of the zero-quantum T_2 is inhomogeneous broadening resulting from a dispersion in chemical shifts. The increase in the lipid line widths at lower temperature without a corresponding decrease in the magnetization exchange rate suggests that the $^{13}C{=}O$ and $^{13}CH_2$ resonances have a significant inhomogeneous contribution. A more accurate estimate of the effective zero-quantum T_2 may be obtained from T_2 measurements in a spin-echo experiment where a train of π-pulses is able to eliminate the inhomogeneous component of the observed line widths. Static spectra of 1-[1-^{13}C],2-[2-^{13}C]DPPC were obtained from 5 to −50 °C using a standard CP sequence with a CPMG echo train following the ^{13}C CP pulse. The Fourier transform of the echo-train signal obtained at −50 °C is shown in Figure 6a. The echo-train line widths for the $^{13}C{=}O$ (90 Hz) and $^{13}CH_2$ (65 Hz) resonances are substantially narrower than those observed under static and MAS conditions and importantly were largely

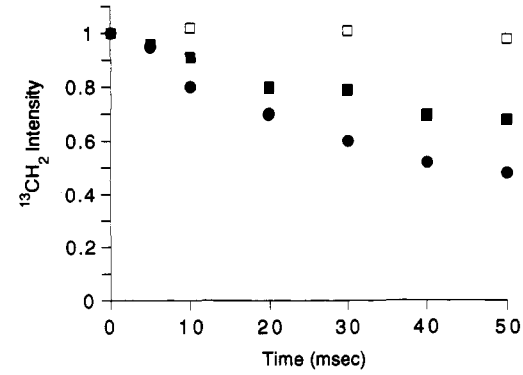

FIGURE 7: Magnetization exchange curves for intermolecular RR measurements in DPPC. Intensity changes are shown for 2-[2-^{13}C]-DPPC that was diluted 1:10 with 2-[1-^{13}C]DPPC (■) and 1,2-[1-^{13}C]DPPC (●). Off rotational resonance data points (□) were obtained for 1,2-[1-^{13}C]DPPC at 9 kHz. The temperature was maintained at −50 °C.

insensitive to the change in temperature. These data argue that an estimate of the zero-quantum T_2 from the linewidths represents a *lower* limit for interpreting the magnetization exchange curves and that for the lipid simulations a zero quantum T_2 closer to 2.1 ms is appropriate for the simulations over the entire temperature range. This longer T_2 value represents an upper limit for the zero-quantum T_2 and translates into a 5.0-Å estimate of the $^{13}C{=}O{\cdots}^{13}CH_2$ internuclear distance (Figure 6b).

The measurement of an internuclear distance in the backbone region of the phospholipid molecule serves to constrain structural models of DPPC in fully hydrated bilayers. In the crystal structure of DMPC-A (Figure 1), the distance between the *sn*-1 C=O and the *sn*-2 CH_2 is 5.5 Å (Pearson & Pascher, 1979). DLPE has a similar crystal structure, and the corresponding distance is 5.7 Å [see Pascher et al. (1992)]. In both lipids the fatty acid chains are displaced by three methylene units (~3.6 Å). A shorter distance between the $^{13}C{=}O$ and $^{13}CH_2$ groups measured by NMR can be rationalized by conformational changes in the glycerol backbone that reduce the axial displacement of the two acyl chains, consistent with neutron diffraction measurements of hydrated phospholipid bilayers that indicate the axial displacement in DPPC is ~1.8 Å (Büldt et al., 1978). Recent solid-state NMR studies of DPPC in the L_α phase suggested that the time-averaged orientation of the glycerol backbone is tilted from the bilayer normal (Smith et al., 1992). The ensemble of L_α phase conformations place the chains more closely in register on average. Solid-state NMR studies are in progress on DMPC to compare directly the NMR and crystal structures. RR measurements on DMPC crystals will generate a set of control curves similar to those obtained with peptide crystals (Peersen et al., 1992) where the internuclear distances are fixed and known independently from the crystal structure. Furthermore, crystal–membrane comparisons should permit a more quantitative estimate of the influence of heterogeneity and lipid dynamics on the RR-driven exchange rates.

Intermolecular RR NMR Measurements. One of the long-range aims of our RR NMR studies is to be able to determine the relative location and orientation of different membrane components and to characterize specific membrane interactions. In this section, we demonstrate that both lipid–lipid and lipid–protein distances can be estimated from intermolecular RR NMR measurements. Figure 7 presents magnetization exchange curves for intermolecular RR measurements in DPPC. Intensity changes are shown for 2-[2-^{13}C]DPPC

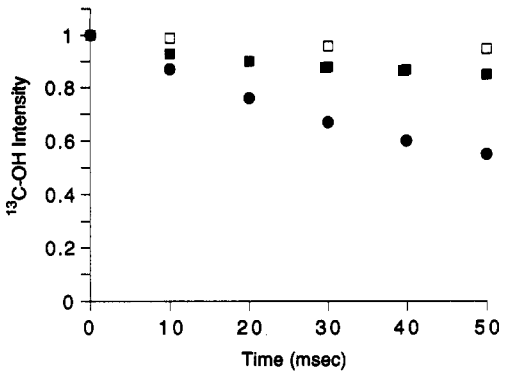

FIGURE 8: Magnetization exchange curves of [^{13}C–OH Y_{93}]GPA-TM in 1,2-[2-^{13}C]DPPC (●). The MAS speed was set to 11 020 Hz, corresponding to the $n = 1$ resonance condition for these ^{13}C labels. The magnitude of magnetization exchange is clearly greater than is observed off the RR condition (□) and for the ^{13}C–OH labeled peptide reconstituted into unlabeled DMPC (■). The temperature was maintained at −50 °C.

that has been diluted 1:10 with 2-[1-^{13}C]DPPC (■) or 1,2-[1-^{13}C]DPPC (●). In these experiments, the more abundant 1-^{13}C label was selectively inverted and *only* the intensity of the 2-^{13}C resonance was monitored. The 2-^{13}C resonance undergoes large intensity changes and serves as a "probe" label in a sea of 1-^{13}C-labeled lipids. In contrast to the intramolecular experiments described above, there are no unique isolated pairs of labels and consequently the exchange curves do not correspond to a specific internuclear distance. These are comparative experiments. The observation of significant magnetization exchange between the 1-^{13}C and 2-^{13}C labels on different lipid molecules in the on-RR curves *relative to* that in the off-RR curves demonstrates that these sites are in close proximity. Similar results were obtained using 2-[1-^{13}C] diluted 1:10 into 2-[2-^{13}C] and 1,2-[2-^{13}C] (data not shown). On the basis of the intramolecular measurements, the magnitude of RR-driven exchange indicates that the average distance between these labels is on the order of 4–5 Å. Comparison of the single- and double-labeled experiments adds support to the conclusion that the 1- and 2-^{13}C sites on neighboring lipids are close in space. These experiments demonstrate that intermolecular measurements are possible.

Intermolecular magnetization exchange rates have also been measured between ^{13}C-labeled DPPC and a ^{13}C–OH tyrosine label on a hydrophobic peptide corresponding to the transmembrane domain of glycophorin A (GPA-TM). As above, the ^{13}C labels are near the membrane interface. Tyrosine 93 (where the numbering reflects the sequence of native glycophorin) is three amino acids from arginine 96, which marks the end of the transmembrane domain. We demonstrate in the following paper that the GPA-TM domain through G_{94} remains helical (Smith et al., 1994). Figure 8 presents magnetization exchange curves of [^{13}C–OH Y_{93}]GPA-TM in 1,2 -[2-^{13}C]DPPC. In these experiments, the lipid CH_2 resonance at 34 ppm was inverted and the tyrosine resonance at 156 ppm was monitored as a function of the RR mix time. The chemical shift of the tyrosine resonance is typical of a protonated ^{13}C–OH sidechain. The MAS speed was set to 11 020 Hz, corresponding to the $n = 1$ resonance condition for these ^{13}C labels. A decrease in tyrosine ^{13}C–OH intensity (●) is clearly observed and is consistent with an average distance between the two ^{13}C sites of 4–5 Å. The magnitude of magnetization exchange is clearly greater than that observed off the RR condition(□) and for the ^{13}C–OH labeled peptide reconstituted into unlabeled DMPC (■).

As in the lipid–lipid magnetization exchange experiments, the lipid–tyrosine data do not yield a specific internuclear distance since there are likely to be an ensemble of distances or structures that generate the observed exchange curve. However, the data constrain the position of the tyrosine ^{13}C–OH to be near the lipid acyl chain carbonyls and raise the possibility that these groups are hydrogen bonded in membranes. Reithmeier and co-workers (Landolt-Marticorena et al., 1993) have analyzed the distribution of amino acids in the transmembrane segments of human type I single-span membrane proteins. Their results clearly show that the aromatic residues tyrosine and tryptophan occur preferentially at the cytoplasmic boundary and are excluded from the interior of these transmembrane sequences, as is the case with glycophorin A. In contrast, serine is randomly distributed and is not strongly excluded from the hydrophobic core of the transmembrane domain. Tyrosine and serine both have hydroxyl functional groups and are generally placed in the middle of hydropathy scales based on the partitioning of amino acid side chains between water and nonpolar environments (Engelman et al., 1986). Serine has the potential to hydrogen bond back to the backbone in helical geometries, which may make this residue effectively more hydrophobic (Engelman et al., 1986). The tyrosine hydroxyl is only capable of intermolecular hydrogen bonding, and the aromatic system may make the side chain more polar than is suggested by various hydropathy scales (Cozzi et al., 1993). The mutagenesis studies of Lemmon et al. (1992) on glycophorin A support this idea, since tyrosine substitutions are shown to disrupt dimerization even at those positions (e.g., A_{82}) not thought to be in the dimer interface, whereas similar substitutions with serine have no influence on dimer formation.

CONCLUSIONS

In summary, RR NMR methods are shown to be effective for determining intramolecular and intermolecular distances between ^{13}C-labeled sites in hydrated membranes. Hydration of phospholipids is known to have a critical influence on lipid structure, and the intramolecular NMR measurements are consistent with the acyl chains of DPPC being closer in register in hydrated membranes than in the crystal structure of DMPC. This difference in conformation allows the acyl chain carbonyls to be more equivalently positioned at the membrane interface. The intermolecular distance measurements are shown to be effective for defining the relative orientation and location of membrane lipids and peptides in bilayers. The RR NMR studies on glycophorin–lipid interactions indicate that Y_{93} is oriented toward the surrounding lipids and near the membrane interface. These results, along with measurements of the protein secondary structure in the following paper (Smith et al., 1994), provide direct constraints on the structure of the glycophorin transmembrane domain in membrane bilayers.

ACKNOWLEDGMENT

We gratefully acknowledge Dr. Raj Betageri for the *t*-Boc chemistry, Martine Ziliox for obtaining the high-power proton-decoupling series, and Malcolm Levitt and Bob Griffin for the original and updated versions of the CC2Z simulation program. We also thank Jake Schaefer, Olve Peersen, and Günther Metz for numerous discussions about the RR experiments and simulations, and Irina Kustanovich for her assistance in the preliminary intermolecular RR NMR studies on DPPC.

REFERENCES

Bormann, B. J., Knowles, W. J., & Marchesi, V. T. (1989) *J. Biol. Chem. 264*, 4033–4037.

Büldt, G., Gally, H. U., Seelig, A., Seelig, J., & Zaccai, G. (1978) *Nature 271*, 182–184.

Cozzi, F., Cinquini, M., Annuziata, R., & Siegel, J. S. (1993) *J. Am. Chem. Soc. 115*, 5330–5331.

Eklund, K. K., Virtanen, J. A., Kinnunen, P. K., Kasurinen, J., & Somerharju, P. J. (1992) *Biochemistry 31*, 8560–8565.

Engelman, D. M., Steitz, T. A., & Goldman, A. (1986) *Annu. Rev. Biophys. Biophys. Chem. 15*, 321–353.

Furthmayr, H., & Marchesi, V. T. (1976) *Biochemistry 15*, 1137–1144.

Garroway, A. N. (1977) *J. Magn. Reson. 28*, 365–371.

Griffin, R. G. (1981) *Methods Enzymol. 72*, 108–174.

Haberkorn, R. A., Stark, R. E., van Willigen, H., & Griffin, R. G. (1981) *J. Am. Chem. Soc. 103*, 2534–2539.

Hartzell, C. J., Whitfield, M., Oas, T. G., & Drobny, G. P. (1987) *J. Am. Chem. Soc. 109*, 5966–5969.

Kubo, A., & McDowell, C. A. (1988) *J. Chem. Soc., Faraday Trans. 1: 84*, 3713–3730.

Landolt-Marticorena, C., Williams, K. A., Deber, C. M., & Reithmeier, R. A. F. (1993) *J. Mol. Biol. 229*, 602–608.

Lemmon, M. A., Flanagan, J. M., Hunt, J. F., Adair, B. D., Bormann, B. J., Dempsey, C. E., & Engelman, D. M. (1992a) *J. Biol. Chem. 267*, 7683–7689.

Lemmon, M. A., Flanagan, J. M., Treutlein, H. R., Zhang, J., & Engelman, D. M. (1992b) *Biochemistry 31*, 12719–12725.

Levitt, M. H., Raleigh, D. P., Creuzet, F., & Griffin, R. G. (1990) *J. Chem. Phys. 92*, 6347–6364.

Nagle, J. F., & Wilkinson, D. A. (1982) *Biochemistry 21*, 3817–3821.

Nakashima, H., & Nishikawa, K. (1992) *FEBS Lett. 303*, 141–146.

Oas, T. G., Hartzell, C. J., McMahon, T. J., Drobny, G. P., & Dahlquist, F. W. (1987) *J. Am. Chem. Soc. 109*, 5956–5962.

Pascher, I., Lundmark, M., Nyholm, P.-G., & Sundell, S. (1992) *Biochim. Biophys. Acta 1113*, 339–373.

Pearson, R. H., & Pascher, I. (1979) *Nature 281*, 499–501.

Peersen, O. B., & Smith, S. O. (1993) *Concepts Magn. Reson. 5*, 305–317.

Peersen, O. B., Yoshimura, S., Hojo, H., Aimoto, S., & Smith, S. O. (1992) *J. Am. Chem. Soc. 114*, 4332–4335.

Peersen, O. B., Wu, X., Kustanovich, I., & Smith, S. O. (1993) *J. Magn. Reson. 104*, 334–339.

Peersen, O. B., Wu, X., & Smith, S. O. (1994) *J. Magn. Reson. 106*, 127–131.

Raleigh, D. P., Levitt, M. H., & Griffin, R. G. (1988) *Chem. Phys. Lett. 146*, 71–76.

Roeske, R. (1963) *J. Org. Chem. 28*, 1251–1253.

Ruocco, M. J., & Shipley, G. G. (1982) *Biochim. Biophys. Acta 684*, 59–66.

Smith, S. O., & Peersen, O. B. (1992) *Annu. Rev. Biophys. Biomol. Struct. 21*, 25–47.

Smith, S. O., Kustanovich, I., Bhamidipati, S., Salmon, A., & Hamilton, J. A. (1992) *Biochemistry 31*, 11660–11664.

Smith, S. O., Jonas, R., Braiman, M., & Bormann, B. J. (1994) *Biochemistry* (following paper in this issue).

Thompson, L. K., McDermott, A., Raap, J., van der Wielen, C. M., Lugtenburg, J., Herzfeld, J., & Griffin, R. G. (1992) *Biochemistry 31*, 7931–7938.

Treutlein, H. R., Lemmon, M. A., Engelman, D. M., & Brünger, A. T. (1992) *Biochemistry 31*, 12726–12733.